# Stoichiometry of the Interaction of Prostaglandin H Synthase with Substrates†

Ah-Lim Tsai, Gang Wu, and Richard J. Kulmacz*

*Division of Hematology, Department of Internal Medicine, University of Texas Health Science Center at Houston, 6431 Fannin Street, Houston, Texas 77030*

*Received February 20, 1997; Revised Manuscript Received August 14, 1997*⊗

ABSTRACT: Prostaglandin H synthase (PGHS) catalyzes both peroxidase and cyclooxygenase reactions. Resolution of several current issues regarding the PGHS catalytic mechanism hinges on the stoichiometry of the reaction of PGHS with hydroperoxide, fatty acid, and oxygen. The dependence of wide-doublet tyrosyl radical accumulation in PGHS isoform 1 on hydroperoxide stoichiometry, has been determined; this catalytically active radical is formed efficiently at stoichiometries ≤1 after only 300 ms of reaction. This is consistent with intramolecular formation of the radical from PGHS Compound I but inconsistent with an alternative pathway involving reduction of Compound I to Compound II by a second hydroperoxide molecule. Results from stopped-flow studies indicate that the hydroperoxide level influences the rate of Compound II formation indirectly, via changes in the transient accumulation of Compound I, rather than by reducing Compound I. PGHS and soybean lipoxygenase reactions with 11,14-eicosadienoic acid (20:2) were also analyzed using a spectrophotometer cuvette fitted with an oxygen electrode to monitor lipid product formation and oxygen consumption simultaneously. The results show that the oxygen electrode signal is inherently dampened and thus underestimates the oxygen consumption rate; the discrepancy is much larger for the more rapidly accelerating PGHS reaction than for the lipoxygenase reaction. When correction is made for the electrode dampening, the ratio between the peak rates of oxygen consumption and lipid product formation was near unity for both PGHS and lipoxygenase, indicating a reaction stoichiometry of about 1 mol of $O_2$ consumed/mol of 20:2 oxygenated for both enzymes. Separately, a stoichiometry of 0.9 mol of $O_2$ consumed / mol oxygenated fatty acid was obtained when limiting amounts of 20:2 were reacted to completion with excess PGHS; the corresponding stoichiometry with arachidonic acid was 1.9. These $O_2$/fatty acid stoichiometries are consistent with a dioxygenase mechanism for reaction of PGHS with both fatty acids and inconsistent with a mixed dioxygenase/monooxygenase mechanism proposed for the reaction with 20:2. The present conclusions reduce the complexity of the mechanisms that need to be considered for PGHS catalysis.

Prostaglandin H synthase (PGHS[1]) has two enzymatic activities involving four substrates. The peroxidase activity of PGHS reduces a hydroperoxide, such as $PGG_2$, to the corresponding alcohol, such as $PGH_2$, with concomitant oxidation of a reducing cosubstrate. In the cyclooxygenase reaction, molecular oxygen is inserted into a polyunsaturated fatty acid; with arachidonic acid, the product is $PGG_2$. Although enzymatic and crystallographic studies have shown that the peroxidase and cyclooxygenase active sites are physically distinct (*1*, *2*), there is considerable evidence that peroxidase intermediates are involved in cyclooxygenase catalysis (*3*). Reaction of PGHS with hydroperoxide rapidly produces oxidized peroxidase intermediates and a tyrosyl radical with a strained conformation of the phenyl ring (*4*). This tyrosyl radical can abstract a hydrogen atom from arachidonate bound in the cyclooxygenase site to form an arachidonyl radical, a step that is believed to be rate limiting for cyclooxygenase catalysis (*5*). Two basic mechanisms have been proposed to account for the functional connection between peroxidase and cyclooxygenase catalysis. These are a branched-chain mechanism (Scheme 1), which postulates a tyrosyl radical as the central oxidant in the cyclooxygenase reaction (*6*), and an alternative mechanism (Scheme 2) in which the primary cyclooxygenase oxidant is peroxidase Compound I, with a tyrosyl radical playing a secondary role in catalysis (*7*, *8*).

Important questions remain regarding the stoichiometry of the reaction between the enzyme and hydroperoxide leading to catalytically active tyrosyl radical formation. In the branched-chain mechanism (*6*), formation of the radical requires an initial interaction with a single equivalent of hydroperoxide followed by an intramolecular electron transfer (steps a and d in Scheme 1). Compound I is postulated as the precursor of the radical rather than Compound II because radical formation is accompanied by formation of the ferryl, not the ferric, state of heme (*4*). In the alternative mechanism (*7*−*9*), the active tyrosyl radical is formed in three steps, requiring reduction of Compound I to Compound II by a second molecule of hydroperoxide (steps a, f, and g in Scheme 2). The two mechanisms thus differ in the number of interactions with hydroperoxide required for formation of the active radical. To address this issue, we have examined the effect of limiting hydroperoxide on the tyrosyl radical intensity in PGHS isoform 1, and we also have characterized the interaction of Compound I with

† This work was supported in part by NIH Grants GM 44911 (A.-L.T.) and GM 52170 (R.J.K.).

* Author to whom correspondence should be addressed [telephone (713) 500-6772; fax (713) 500-6810; e-mail kulmacz@heart.med.uth.tmc.edu].

⊗ Abstract published in *Advance ACS Abstracts,* October 1, 1997.

[1] Abbreviations: PGHS, prostaglandin H synthase isoform 1; 20:4, arachidonic acid; 20:2, *cis,cis*-11,14-eicosadienoic acid; MCPBA, *m*-chloroperoxybenzoic acid; EtOOH, ethyl hydrogen peroxide.

S0006-2960(97)00397-8 CCC: $14.00 

Scheme 1: Branched-Chain Mechanism for PGHS Based on Proposal by Dietz et al. (*6*)[a]

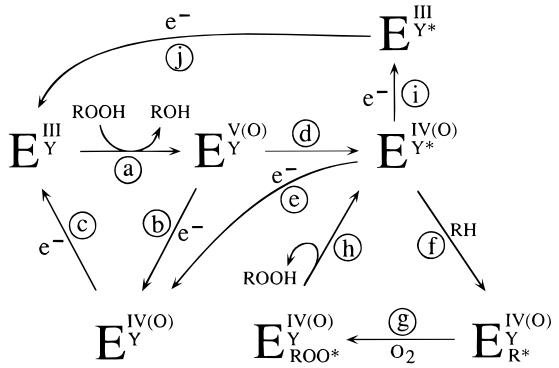

[a] The formal oxidation states of the heme and the status of Y385 are indicated for each enzyme intermediate. EIII/Y, resting ferric enzyme; EV(O)/Y, Compound I; EIV(O)/Y, Compound II; EIV(O)/Y*, catalytically active wide-doublet tyrosyl radical; EIV(O)/Y/R*, PGHS with bound arachidonyl radical; EIV(O)/Y/ROO*, PGHS with bound fatty acid hydroperoxyl radical; EIII/Y*, tyrosyl radical with ferric heme; RH, fatty acid; ROOH, fatty acid hydroperoxide; ROH, hydroxy fatty acid; and $e^-$, reducing equivalent.

Scheme 2: Alternative Mechanism for PGHS Based on Proposals by Bakovic and Dunford (*7*−*9*, *18*)[a]

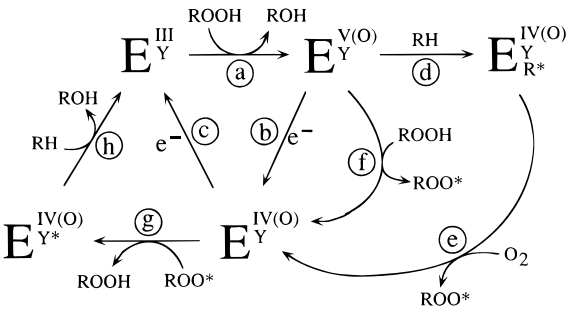

[a] The formal oxidation states of the heme and the status of Y385 are indicated for each enzyme intermediate. EIII/Y, resting ferric enzyme; E(O)/Y, Compound I; EIV(O)/Y/R*, PGHS with bound arachidonyl radical; EIV(O)/Y, Compound II; EIV(O)/Y*, catalytically active wide-doublet tyrosyl radical; RH, fatty acid; ROOH, fatty acid hydroperoxide; ROH, hydroxy fatty acid; ROO*, fatty acid hydroperoxyl radical; and $e^-$, reducing equivalent. Reactions with 20:2 and 20:4 were proposed to involve analogous reaction steps except for step h, which was examined for 20:2 but not for 20:4 (*9*).

hydroperoxide. The results indicate that formation of the tyrosyl radical requires only one interaction with hydroperoxide and that hydroperoxides increase the rate of Compound II formation indirectly.

The stoichiometry among other PGHS substrates (i.e., fatty acid, oxygen, and reducing cosubstrate) has been a crucial element in the development and evaluation of reaction mechanisms (*10*, *11*). Recently, the observed stoichiometry between fatty acid and oxygen consumption furnished the basis for proposing a novel monooxygenase step (step h in Scheme 2) in the reaction of PGHS with 20:2 (*7*, *9*). An ability of PGHS to act as a monooxygenase as well as a dioxygenase with 20:2 would raise many questions about current concepts of the PGHS reaction mechanism with other fatty acids, including arachidonic acid. The accuracy of stoichiometric measurements has been contentious in past comparisons of reaction mechanisms, in part because pairs of substrates were monitored in parallel reactions rather than in the same vessel. Spectrophotometric measurements have been used to determine the kinetics of fatty acid oxygenation and cosubstrate oxidation, whereas separate polarographic measurements were used to obtain detailed information about the kinetics of oxygen consumption. In addition, the complex nature of polarographic oxygen measurement has not always been appreciated fully. This has made it difficult to evaluate the reliability of key stoichiometric ratios involving oxygen uptake. The present studies use simultaneous spectrophotometric and polarographic measurements to address the oxygen/fatty acid stoichiometric issue. The results reveal that the polarographic electrode responses markedly underestimate the velocities of rapidly accelerating reactions such as PGHS cyclooxygenase catalysis. The corrected substrate stoichiometry is consistent with a conventional dioxygenase mechanism for reaction of PGHS with 20:2.

## MATERIALS AND METHODS

Arachidonic acid and 20:2 were obtained from NuChek Labs. MCPBA was from Aldrich Chemical and EtOOH from Polyscience. EtOOH concentrations were quantified using a molar absorption coefficient of 43 $M^{-1}$ $cm^{-1}$ at 230 nm. Hydroquinone was from MCB. Soybean lipoxygenase, potassium ferricyanide, and heme were from Sigma. PGHS (isoform 1) was purified from ovine seminal vesicles as the apoenzyme (*12*). PGHS was reconstituted with heme (*13*), and the holoenzyme concentration was determined from the absorbance at 410 nm and an absorption coefficient of 165 $mM^{-1}$ $cm^{-1}$.

Tyrosyl radical accumulation was assessed by EPR measurements. For longer reactions, 0.1−10 equiv of EtOOH in a small volume of water was mixed manually with PGHS in quartz cuvettes at 0 °C and reacted for 6−8 s before freezing in a dry ice/acetone bath (*13*). Short reactions used an Update Instruments (Madison, WI) System 1000 chemical/freeze quench apparatus to deliver equal volumes of PGHS (in 0.2 M potassium phosphate, pH 7.2, with 0.1% Tween 20 and 15% glycerol) and EtOOH (in water) to a Wiskind 4-grid mixer connected to a 300 ms aging tube. All fluid components were immersed in an ice bath. The mixture emerging from the aging tube was sprayed into isopentane chilled at −130 °C to stop the reaction, and the crystals were packed into a quartz EPR cuvette. A packing factor of about 0.5 was measured under the same conditions with standard myoglobin or cupric sulfate solutions. All EPR samples were stored in liquid nitrogen until analyzed. EPR spectra were recorded on a Varian E-6 spectrometer at 90 K; spin concentrations were determined by double integration using a copper sulfate standard (*13*). The microwave power was 1 mW, and the modulation was 3.2 G.

Transient kinetic studies were conducted on an Applied Photophysics stopped-flow instrument with SX18MV software package using either the single or the sequential mixing mode. A static spectrum (350−550 nm) was recorded after each sequential mixing reaction, and the absorbance at 510 nm (an isosbestic point between resting enzyme and enzyme with bleached heme) was used to correct for drifting of the baseline. Computer simulations were performed by numerical integration using the SCoP program (Simulation Resources) as described previously (*11*).

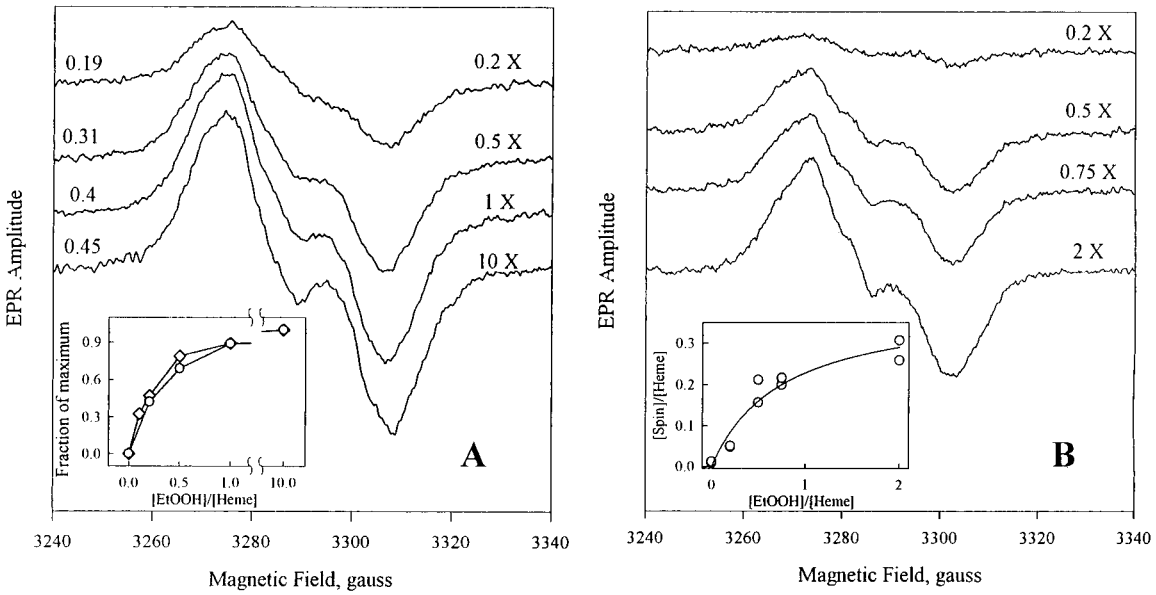


FIGURE 1: Effect of EtOOH stoichiometry on tyrosyl radical formation. (A) EPR spectra were recorded after PGHS holoenzyme (10 $\mu$M heme) was manually mixed with various levels of EtOOH and reacted at 0 °C for 6−8 s. Spectra are shown for one of the two batches of PGHS examined. The EtOOH/heme ratios are given on the right side of each spectrum, and the radical intensities (in spins/heme) are shown on the left side. (Inset) The radical intensities obtained with both batches of PGHS (normalized to the intensity of the sample reacted with 10 equiv of EtOOH) are shown as a function of the hydroperoxide stoichiometry. (B) EPR spectra were recorded after PGHS holoenzyme (30.9 $\mu$M heme) was mixed with an equal volume of various levels of EtOOH, reacted at 0 °C for 300 ms, and trapped in isopentane chilled at −130 °C. Spectra are shown for one of the duplicate samples. The EtOOH/heme ratios are given on the right side of each spectrum. (Inset) The radical intensities are shown as a function of the hydroperoxide stoichiometry. Details are given under Materials and Methods.

Oxygen consumption was measured with one of two polarographic oxygen electrodes. A YSI Model 5331 electrode and a Model 53 monitor were used in standard assays (*12*). An Instech Labs Model 203 amplifier and a Model 125 electrode in a custom Delrin holder, enclosing a reaction volume of 2.8 mL, were used for oxygen measurements in a 1 cm path length spectrophotometer cuvette. The cuvette was continuously stirred with a 1.5 × 7 mm Teflon-coated magnet driven by an Instech Model 604 magnetic stir motor mounted near the side wall of the cuvette. The temperature was maintained at 25 °C by water circulated through a jacketed cell holder in a Shimadzu Model 2101 PC spectrophotometer. The amplified oxygen electrode signal was digitized and stored using a Remote Measurement Systems Model ADC-1 A/D converter connected to a Macintosh SE computer. The electrode signal was calibrated for oxygen concentration on the basis of the assay described by Robinson and Cooper (*14*). Correction of the electrode signal for dampening by the polyethylene membrane protecting the electrode surface used the formula described previously (*11*).

Oxygen consumption stoichiometries for 20:2 and 20:4 with PGHS or soybean lipoxygenase were determined by incubating enzyme with limiting amounts of fatty acid and allowing reaction to proceed to completion (at least 90 s). Additional enzyme or hydrogen peroxide (100 $\mu$M) was added near the end of each reaction to ensure that sufficient activated enzyme remained to exhaust the fatty acid. The oxygen concentration did not change when PGHS was incubated with hydrogen peroxide in the absence of fatty acid or when fatty acid was incubated with hydrogen peroxide in the absence of enzyme. Oxygen levels were measured with the YSI electrode and monitor. With these prolonged incubation times, membrane dampening (relaxation rate constant of about 0.25 $s^{-1}$) is not a significant factor, and the electrode signal provides an accurate indication of the true oxygen concentration. The reaction buffer for PGHS was 0.1 M potassium phosphate, pH 7.2, with 1 mM phenol, and that for soybean lipoxygenase was 0.1 M Tris, pH 8.5; the temperature was maintained at 30 °C.

## RESULTS AND DISCUSSION

*Stoichiometry between Hydroperoxide and Tyrosyl Radical Formation.* Reaction of PGHS with hydroperoxide forms a wide-doublet tyrosyl radical which appears to be a competent oxidant for cyclooxygenase catalysis (*4*−*6*, *15*). The stoichiometric relationship between hydroperoxide consumption and tyrosyl radical formation was investigated by quantitation of the radical intensity after reaction of PGHS with limiting amounts of EtOOH. In manually mixed reactions lasting 6−8 s, the tyrosyl radical was observed even at 0.1 EtOOH/heme, the lowest ratio tested (Figure 1A). The intensity of the radical initially increased in proportion to the added hydroperoxide and then leveled off above an EtOOH/heme ratio of 1.0 (Figure 1A, inset). Although the absolute peak concentration of the radical varied between the PGHS preparations examined, the response of radical intensity to the hydroperoxide stoichiometry was quite reproducible (Figure 1A, inset).

Rapid-freezing techniques were used to monitor the formation of tyrosyl radical at shorter reaction times than possible with the manual method. In reaction of PGHS with 2 equiv of EtOOH at 0 °C, the wide-doublet tyrosyl radical was formed at the earliest time point tested (38 ms) and its intensity was maximal by 300 ms (data not shown). The effect of peroxide stoichiometry on radical formation was therefore examined after 300 ms of reaction (Figure 1B). Detectable wide-doublet tyrosyl radical was generated at the lowest peroxide/heme ratio tested, 0.2, and the radical intensity increased in a saturable fashion as the peroxide was

increased, leveling off at peroxide/heme ratios >1 (Figure 1B, inset). The present results at both short and moderate reaction times are consistent with an earlier observation that the wide-doublet radical intensities in reactions of PGHS with 2 or 5 equiv of EtOOH were not much larger than that with 1 equiv of EtOOH (*4*). These results demonstrate clearly that interaction of PGHS with about 1 equiv of hydroperoxide is sufficient to generate near-maximal levels of the catalytically active tyrosyl radical in as little as 300 ms.

*Computer Simulation of Tyrosyl Radical Accumulation during Reaction with EtOOH.* The kinetics of tyrosyl radical formation expected for the branched-chain mechanism (Scheme 1) and the alternative mechanism (Scheme 2) were predicted by numerical integration. For the branched-chain mechanism, the simulations were based on the PGHS peroxidase mechanism proposed by Dietz et al. (*6*), with the following steps (shown as steps a−e, i, and j in Scheme 1):

$$\text{E(III)} + \text{ROOH} \rightarrow \text{E(V)} + \text{ROH} \quad (1)$$

$$\text{E(V)} + \text{Red}_e \rightarrow \text{E(IV)} + \text{Ox}_e \quad (2)$$

$$\text{E(IV)} + \text{Red}_e \rightarrow \text{E(III)} + \text{Ox}_e \quad (3)$$

$$\text{E(V)} \rightarrow \text{E(IV)-Y*} \quad (4)$$

$$\text{E(IV)-Y*} + \text{Red}_e \rightarrow \text{E(IV)} + \text{Ox}_e \quad (5)$$

$$\text{E(IV)-Y*} + \text{Red}_e \rightarrow \text{E(III)-Y*} + \text{Ox}_e \quad (6)$$

$$\text{E(III)-Y*} + \text{Red}_e \rightarrow \text{E(III)} + \text{Ox}_e \quad (7)$$

In eq 1 the resting enzyme [shown as E(III) to reflect the formal oxidation state of the heme] reacts with hydroperoxide (ROOH) to form Intermediate I [E(V), equivalent to Compound I] and the alcohol (ROH). The second-order rate constant of $3 \times 10^6$ $M^{-1}$ $s^{-1}$ used for this step was based on measurements at 1 °C (*16*). Intermediate I can then undergo an internal electron transfer from a tyrosyl residue to form a tyrosyl radical [E(IV)-Y*] in eq 4; a rate constant of 68 $s^{-1}$ was determined for this reaction (*16*). Intermediate I can also react with endogenous reductant ($Red_e$, described in more detail in a later section) to form Compound II [E(IV)] in eq 2. PGHS was assumed to contain 10 equiv of endogenous reductant (see below). The ferryl heme in Compound II and in the tyrosyl radical can undergo one-electron reductions with endogenous reductant (eqs 3 and 6); a rate constant of $1 \times 10^5$ $M^{-1}$ $s^{-1}$ for these steps was based on values for reaction of Compound II with exogenous reductants (*17*). The rate constant for eq 2 was set 5-fold higher than those for eqs 3 and 6 to reflect the expected faster reaction of Compound I than Compound II with reductant. Reduction of the radical center to tyrosine (eqs 5 and 7) was considered separately from heme reduction and was assigned a rate constant of 7 $M^{-1}$ $s^{-1}$ on the basis of the observed slow dissipation of the radical in the absence of added cosubstrate (*15*).

For the alternative mechanism, the simulation of tyrosyl radical kinetics was based on proposals by Bakovic and Dunford (*7*−*9*, *18*), which are shown as steps a, f, and g in Scheme 2 and as eqs 8−10 below:

$$\text{E(III)} + \text{ROOH} \rightarrow \text{E(V)} + \text{ROH} \quad (8)$$

$$\text{E(V)} + \text{ROOH} \rightarrow \text{E(IV)} + \text{ROO*} \quad (9)$$

$$\text{E(IV)} + \text{ROO*} \rightarrow \text{E(IV)-Y*} + \text{ROOH} \quad (10)$$

In eq 8 the resting enzyme [E(III)] reacts with hydroperoxide (ROOH) to form Compound I [E(V)] and alcohol (ROH). This is the same reaction as in eq 1 above, and the same rate constant was used ($3 \times 10^6$ $M^{-1}$ $s^{-1}$). Compound I is reduced by a second molecule of hydroperoxide to form Compound II [E(V)] and a hydroperoxy radical (ROO*) in eq 9. Finally, Compound II reacts in eq 10 with the hydroperoxy radical to form the tyrosyl radical [E(IV)-Y*] and regenerate the hydroperoxide. The absorbance measurements used by Bakovic and Dunford (*8*) did not distinguish between E(IV) and E(IV)-Y*, so it is not known whether eq 9 or eq 10 is rate-limiting for formation of E(IV)-Y*. To maximize the rate of tyrosyl radical formation in the simulations, the overall rate constant reported by Bakovic and Dunford (*8*) for EtOOH, $4.5 \times 10^4$ $M^{-1}$ $s^{-1}$, was used for eq 9 and a high value, $3 \times 10^6$ $M^{-1}$ $s^{-1}$, was used as the rate constant for eq 10. To maximize accumulation of the tyrosyl radical, endogenous reductant was not considered in the simulation of the alternative mechanism.

Numerical integration was performed for each equation set to obtain predictions of the tyrosyl radical concentration as a function of time at several levels of EtOOH (Figure 2). With the branched-chain mechanism, tyrosyl radical accumulation was rapid, reaching a plateau after about 300 ms (Figure 2A). The predicted yield of radical increased with the peroxide stoichiometry, from 0.12 spin/heme at 0.2 equiv of EtOOH to 0.47 spin/heme at 0.75 equiv of EtOOH, and approached a maximal value by just above 2 equiv of EtOOH. This prediction of rapid and efficient radical generation reflects the direct path to the tyrosyl radical in the branched-chain mechanism, requiring only one interaction with hydroperoxide and an intramolecular electron transfer (eqs 1 and 4).

For the alternative mechanism, however, tyrosyl radical accumulation was predicted to be considerably slower, especially at peroxide stoichiometries <1 (Figure 2B). After 8 s of reaction, the predicted radical yield was essentially zero with up to 0.75 equiv of EtOOH and only 0.05 spin/heme with 1 equiv of EtOOH. For reaction times <1 s, peroxide/heme ratios of >1 were needed to produce significant yields of radical. The prediction of inefficient and slow tyrosyl radical formation with the alternative mechanism reflects the requirement for two serial interactions of enzyme with hydroperoxide prior to tyrosyl radical formation (eqs 8 and 9). Under conditions where ≤1 equiv of hydroperoxide is added, only a statistically small fraction of enzyme has more than one interaction with hydroperoxide early in the reaction, making the rate of tyrosyl radical formation and hydroperoxide regeneration (eq 10) very slow. When ∼2 equiv of hydroperoxide is added, ∼1 equiv of unreacted hydroperoxide is immediately available for the reaction in eq 9, and tyrosyl radical is predicted to form much more rapidly.

The simulations in Figure 2 show that the two mechanisms predict very different accumulations of tyrosyl radical with

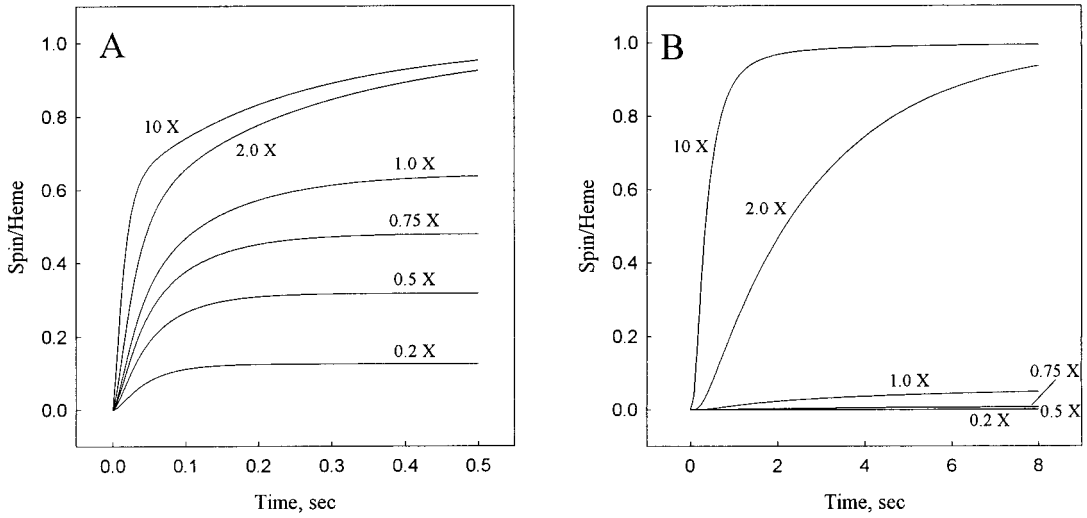


FIGURE 2: Computer simulation of tyrosyl radical accumulation during reaction of PGHS with EtOOH for the branched-chain (Scheme 1) and the alternative (Scheme 2) mechanisms. Numerical integration of rate equations based on the branched-chain mechanism (A) or the alternative mechanism (B) was used to predict the tyrosyl radical concentration as a function of time after PGHS (10 $\mu$M heme) was reacted with EtOOH at the indicated EtOOH/heme ratios. Note the 16-fold difference in the time scales of the two panels. Details are given in the text.

the peroxide stoichiometries and reaction times used in the experiments in Figure 1. The observation of significant radical formation after as little as 300 ms of reaction with substoichiometric peroxide (Figure 1) is clearly consistent with the predicted behavior of the branched-chain mechanism (Figure 2A) and clearly at odds with the predicted behavior of the alternative mechanism (Figure 2B). Thus, the postulated reduction of Compound I by a second equivalent of hydroperoxide and the subsequent oxidation of Compound II by the hydroperoxyl radical (Scheme 2) are almost certainly not involved in the formation of the catalytically active tyrosyl radical. The observed peak radical accumulation at saturating peroxide was considerably lower than the quantitative levels predicted by either mechanism (Figures 1 and 2), probably because neither mechanism accounts for inactive protein present in PGHS preparations (*27*).

*Kinetics of Oxidized Intermediates during Reaction with Stoichiometric Levels of Hydroperoxide.* When PGHS was reacted with stoichiometric amounts of an organic hydroperoxide, MCPBA, in earlier studies (*8*), the absorbance at 414 nm was found to undergo a rapid decrease to a minimum at 60 ms followed by a slower rebound, with the two phases separated by a "steady-state" period lasting about 20−40 ms. The optical changes were attributed to a rapid initial formation of Compound I and a slower conversion of Compound I to Compound II. Because of the large difference in the rates of the two phases, it was concluded that essentially pure Compound I was present during the steady-state period. A second addition of hydroperoxide during this period was found to increase the rate of Compound II formation, with the increase proportional to the concentration of hydroperoxide in the second reaction. These observations were interpreted to reflect a direct reduction of Compound I to Compound II by hydroperoxide and thus a requirement for interaction with 2 equiv of hydroperoxide (Steps a and f in Scheme 2) to form the catalytically active tyrosyl radical (*8*). This stoichiometry conflicts with the present EPR observations, which showed efficient radical formation with substoichiometric levels of hydroperoxide (Figure 1). Accordingly, we re-examined the formation of oxidized enzyme intermediates in reactions with MCPBA under conditions similar to those used by Bakovic and Dunford (*8*). Our enzyme preparation was found to be stable in the absence of exogenous reductant, and so none was added. The reactions were monitored at 408 and 428 nm, the isosbestic points between Intermediate I (i.e., Compound I) and Intermediate II (i.e., Compound II and the tyrosyl radical species, which have equivalent heme optical characteristics) and between resting enzyme and Intermediate I, respectively (*16*). The isosbestic points at 408 and 428 nm are similar to those observed by others (*6*, *19*); somewhat different isosbestic points have been reported for reactions in the presence of added reductant (*8*). The absorbance at 408 nm thus reflects the concentration of resting enzyme, whereas the absorbance at 428 nm reflects the concentration of Intermediate II.

Reaction of PGHS with 1.3 equiv of MCPBA produced a rapid initial decrease in absorbance at 408 nm, due to conversion of resting enzyme to Intermediate I, and a slower increase in absorbance at 428 nm, due to conversion of Intermediate I to Intermediate II (Figure 3, upper panel). The $A_{408}$ value reached a minimum at about 50 ms of reaction and then rebounded to near the initial value after 5 s (Figure 3, upper panel). Because 408 nm is an isosbestic point between Intermediates I and II, the later increase in $A_{408}$ shows that the resting enzyme is slowly regenerated in the reaction. Similarly, the $A_{428}$ value decreased slowly to its initial level from a peak at about 80 ms. It is clear from these results that formation of Intermediate I and its conversion to Intermediate II were both rapid processes, even in the absence of exogenous cosubstrate. The temporal overlap of the $A_{408}$ and $A_{428}$ changes indicate that considerable formation of Intermediate II had occurred at ~50 ms, the point of maximal Intermediate I formation.

The nature of the enzyme species present at the expected point of maximal Intermediate I accumulation, the $A_{408}$ minimum, was examined further in a sequential mixing experiment. For this, PGHS was first reacted with 1.3 equiv of MCPBA for 50 ms under the same conditions used in the upper panel of Figure 3 and then subjected to a second reaction with either buffer or additional MCPBA (Figure 3, lower panel). Mixing with buffer in the second stage resulted

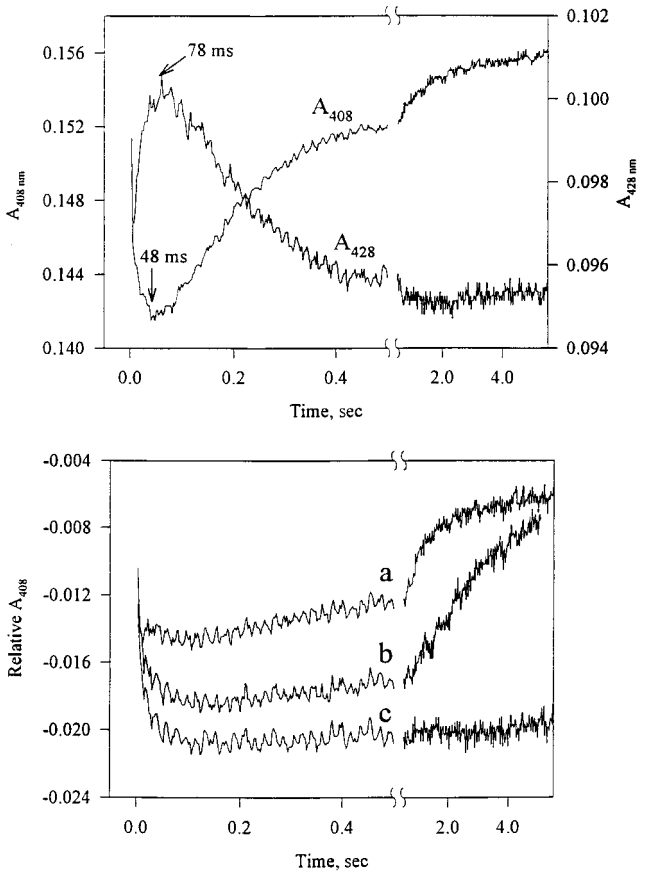


FIGURE 3: Transient kinetics of reactions of PGHS with MCPBA. (Upper panel) Single mixing experiment. The absorbances at 408 and 428 nm were monitored during reaction of PGHS holoenzyme (2 $\mu$M heme) in 50 mM potassium phosphate, pH 7.4, containing 0.04% octyl glucoside and 0.05% Tween 20 with 2.6 $\mu$M MCPBA at 6 ± 1 °C. Each trace represents the average of three reactions. (Lower panel) Sequential mixing experiment. The reaction mixture described for the experiment in panel A was aged for 50 ms before a secondary mixing with an equal volume of buffer (a), 2.6 $\mu$M MCPBA (b), or 3.9 $\mu$M MCPBA (c). Each trace represents the average of two or three reactions. The kinetic data were subtracted from those from a control reaction in which enzyme was mixed with buffer in both the first and second stages. Details are given under Materials and Methods.

in only a slow increase in $A_{408}$ (trace a), reflecting regeneration of resting enzyme, just as expected from the absorbance changes after 50 ms in the single mixing experiment (Figure 3, upper panel). Mixing with a further 2.6 equiv of MCPBA in the second stage, however, led to a rapid further decline in $A_{408}$ followed by a slower recovery of the absorbance (trace b in Figure 3, lower panel). The magnitude of the rapid decrease in $A_{408}$ in the second reaction was comparable to that in the primary reaction with MCPBA (Figure 3, upper panel). The final $A_{408}$ was close to that observed in the buffer control, confirming the eventual return of the enzyme to the resting state and ruling out significant heme destruction or enzyme denaturation. The initial decrease in $A_{408}$ observed in the secondary reaction with 2.6 equiv of MCPBA therefore reflects conversion of resting enzyme to additional Intermediate I, and so considerable resting enzyme was still present before the second reaction with hydroperoxide. Thus, resting enzyme, Intermediate I, and Intermediate II were all present in significant portions at the point of minimal $A_{408}$ in reaction of PGHS with 1.3 equiv of MCPBA. Increasing the MCPBA level in the second-stage reaction to 3.9 equiv produced an even greater initial decrease in $A_{408}$, but there was very little subsequent recovery of absorbance by 5 s (trace c in Figure 3, lower panel), indicating some heme destruction did occur with the higher level of hydroperoxide.

The present re-examination of the reaction of PGHS with stoichiometric levels of MCPBA (Figure 3) suggests a simple explanation for the effect of hydroperoxide on the rate of Intermediate II formation observed by Bakovic and Dunford (*8*). The present observations, under conditions chosen to be similar to those used in the earlier study (*8*), show that conversion of resting enzyme to Compound I never approaches completion at any time during reaction with 1.3 equiv of MCPBA, with a large fraction of enzyme remaining in the resting state even at the point where the $A_{408}$ is at the minimum (Figure 3). Incomplete conversion to Compound I during reaction with 1.3 equiv of MCPBA can be inferred from the spectral changes reported by Bakovic and Dunford (*8*), where the decrease in the absorbance coefficient at 410 nm was only about half that reported earlier for formation of Compound I, both by the same laboratory (*19*) and by others (*6*). Thus, even though formation of Compound I was maximal at the time when the second addition of hydroperoxide was made in the sequential reactions (Figure 3 and ref 8), that maximum fell well short of being quantitative. The large pool of resting enzyme remaining at that point was available to react with the second addition of hydroperoxide to form more Compound I (Figure 3). Bakovic and Dunford (*8*) did not report any observations at 414 nm after the second hydroperoxide addition in their sequential reactions; changes at this wavelength would detect further conversion of resting enzyme to Compound I in their system.

Accumulation of more Compound I upon the second hydroperoxide addition itself increases the rate of Intermediate II formation by the proposed intramolecular mechanism (eqs 2 and 4). The increased rate of Intermediate II formation observed upon a second addition of hydroperoxide (Figure 3 and ref 8) can thus be explained quite adequately as an indirect action. This explanation removes the need for direct reduction of PGHS Compound I by hydroperoxide. Hydrogen peroxide has been reported to reduce myeloperoxidase Compound I to Compound II (*20*), but this may reflect the unusual ability of that particular peroxide to act as reductant as well as oxidant. The same hydroperoxides reported to reduce PGHS Compound I were completely inactive with Compound I of horseradish peroxidase (*8*) which, like PGHS, is a heme peroxidase with bis(histidine) ligation of the heme iron (*21, 22*). The observed PGHS peroxidase reaction kinetics thus remain consistent with the simpler mechanism based on those of horseradish peroxidase and cytochrome *c* peroxidase, with reducing equivalents furnished by endogenous or exogenous electron donors (eqs 1−5 above and steps a−e in Scheme 1).

*Quantitation of Endogenous Reductant.* Regeneration of resting enzyme was consistently observed in reactions of PGHS with <4 equiv of MCPBA (Figure 3) or EtOOH (data not shown), in spite of the absence of added reducing cosubstrate. This pointed to the presence of some endogenous reductant in the purified enzyme. The amount of endogenous reductant was examined by titration of holoenzyme (4.5 $\mu$M heme) with EtOOH in the presence of 0−30 $\mu$M hydroquinone (Figure 4). Hydroquinone and diethyldithiocarbamate both efficiently reduce oxidized PGHS peroxidase intermediates (*17*). Hydroquinone was used in the titrations because it did not react directly with EtOOH

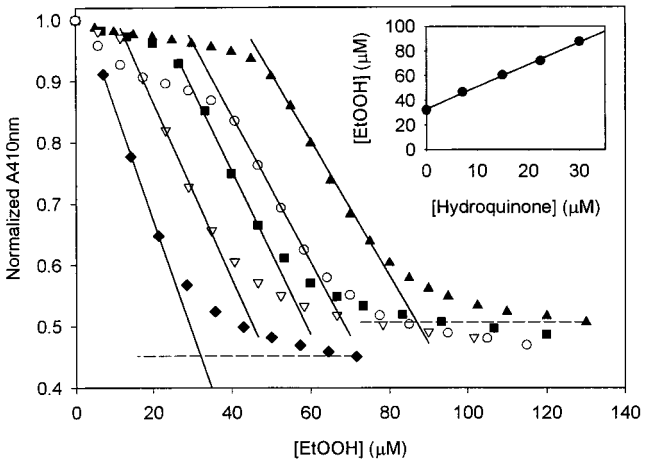


FIGURE 4: Effect of exogenous reductant on bleaching of PGHS heme absorbance by EtOOH. The absorbance at 410 nm was monitored during titration with EtOOH of PGHS holoenzyme (4.5 $\mu$M heme) in 0.1 M potassium phosphate, pH 7.2, containing 0.1% Tween 20 and 0 (◆), 7 (▽), 15 (■), 22 (○), or 30 $\mu$M (▲) hydroquinone in a cuvette thermostated at 25 °C. Incubation was continued after each addition of EtOOH until a stable absorbance was achieved ($\leq$3 min). Endpoints were determined by extrapolation of the central parts of the curves to the final absorbance values, as illustrated for the titrations at 0 and 30 $\mu$M hydroquinone. (Insert) The endpoints from the titrations were plotted as a function of the amount of exogenous reductant. The line was fitted to the data by linear regression.

at a significant rate, in contrast with diethyldithiocarbamate (data not shown). Each addition of EtOOH to native PGHS resulted in transient formation of oxidized intermediates, most of which were spontaneously reduced back to resting enzyme within ~2 min. At equilibrium, though, a fraction of the enzyme did not cycle back, as reflected by the incremental, irreversible decreases in absorbance at 410 nm. After repeated peroxide additions, the absorbance at 410 nm reached a minimum at about half the initial value (Figure 4). In the absence of added reductant, the endpoint in the titration was reached at 32 $\mu$M EtOOH. This corresponds to 7 EtOOH/PGHS heme, in reasonable agreement with the endpoint of 10 EtOOH/PGHS obtained earlier (*4*). The endpoint increased in proportion to the level of hydroquinone initially present, reaching 87 $\mu$M EtOOH with 30 $\mu$M hydroquinone (Figure 4). The presence of hydroquinone resulted in a plateau in the early part of the titration, where EtOOH additions produced relatively small incremental decreases in absorbance (Figure 4). The persistence of this plateau increased in proportion to the hydroquinone level, whereas the slope of the later steep decline in absorbance was little changed. One possible interpretation is that oxidized PGHS intermediates preferentially reacted with hydroquinone, with most heme bleaching occurring when the exogenous reductant was exhausted and the endogenous reductant began to be consumed.

A plot of the titration endpoint as a function of the initial hydroquinone level showed a linear relationship between the two variables (Figure 4, inset). The line fitted to the data had a slope of 1.8 EtOOH/hydroquinone and an intercept of 32 $\mu$M EtOOH. Each mole of hydroquinone thus protected the heme against nearly 2 mol of EtOOH. Because hydroquinone is a two-electron donor, the slope value suggests that only one of the two oxidizing equivalents in EtOOH was involved in bleaching the heme. Dividing the value of the intercept by that of the slope indicates that the endogenous reductant in the enzyme was equivalent to 18 $\mu$M hydroquinone, or about 4 mol hydroquinone/mol of PGHS (8 reducing equiv/mol of PGHS).

The identity of the endogenous electron donor in the purified PGHS that led to the regeneration of resting enzyme (Figures 3 and 4) is not known. Recovery of resting enzyme is not evident in the spectral changes observed by Bakovic and Dunford in the first 200 ms of reaction under similar conditions (*8*). It is possible that the slight differences in buffer composition between the two studies account for the slower regeneration of resting enzyme observed by Bakovic and Dunford (*8*). A simple explanation is that less endogenous reductant was present in their enzyme preparation. A lower level of endogenous reductant may be related to the reported instability of their purified holoenzyme, an instability avoided by addition of a reductant, diethyldithiocarbamate (*8*). Despite the difference in level of endogenous reductant between the present enzyme preparation and that used by Bakovic and Dunford (*8*), it is clear from the discussion above that resting PGHS was incompletely converted to Compound I by stoichiometric amounts of MCPBA in both preparations. Thus, the level of endogenous reductant is unlikely to be a crucial factor determining the yield of Compound I when rapidly reacting hydroperoxides are mixed with PGHS.

The endogenous reductant may also be involved in the spontaneous decay of tyrosyl radical intensity with time (*15*). However, the decay kinetics are very slow compared to the rate of radical formation, and the radical intensities in samples freeze-trapped after short reaction times, as for the experiments in Figure 1, are unlikely to be decreased significantly. In any case, quenching of the radical by endogenous reductant would artificially increase the level of hydroperoxide needed to saturate the radical. Thus, the peroxide stoichiometry observed to saturate the radical is, if anything, an overestimate of the true value, and the conclusions drawn are not affected.

*Simultaneous Spectrophotometric and Polarographic Measurements.* The oxygen electrode response kinetics were examined by injection of an aliquot of anaerobic potassium ferricyanide solution into buffer in an optical cuvette (Figure 5A). Mixing was essentially complete within 1.5 s, as indicated by the rapid change in absorbance at 400 nm due to the injected chromophore. The response from the oxygen electrode was considerably slower, with a lag of almost 2 s and a subsequent relaxation rate of about 0.3 $s^{-1}$. The discrepancy between the absorbance and electrode kinetics can be traced to the slow rate of oxygen transport across the electrode membrane (*23*). When the electrode data were corrected for the membrane dampening, the rate of change in oxygen level closely matched the rate of absorbance change, validating the correction algorithm (Figure 5A).

Simultaneous spectrophotometric and oxygen electrode measurements were made during reaction of soybean lipoxygenase with 20:2 (Figure 5B). Formation of fatty acid hydroperoxide, measured from the increase in absorbance at 235 nm due to the conjugated diene product, accelerated to a peak velocity of 0.9 $\mu$M/s after 4−5 s of reaction. The oxygen consumption rate calculated from the uncorrected electrode signal accelerated more slowly, reaching a peak velocity of about 0.8 $\mu$M/s only after ~9 s of reaction. With correction of the electrode data for membrane dampening, the kinetic profiles for oxygen consumption and diene

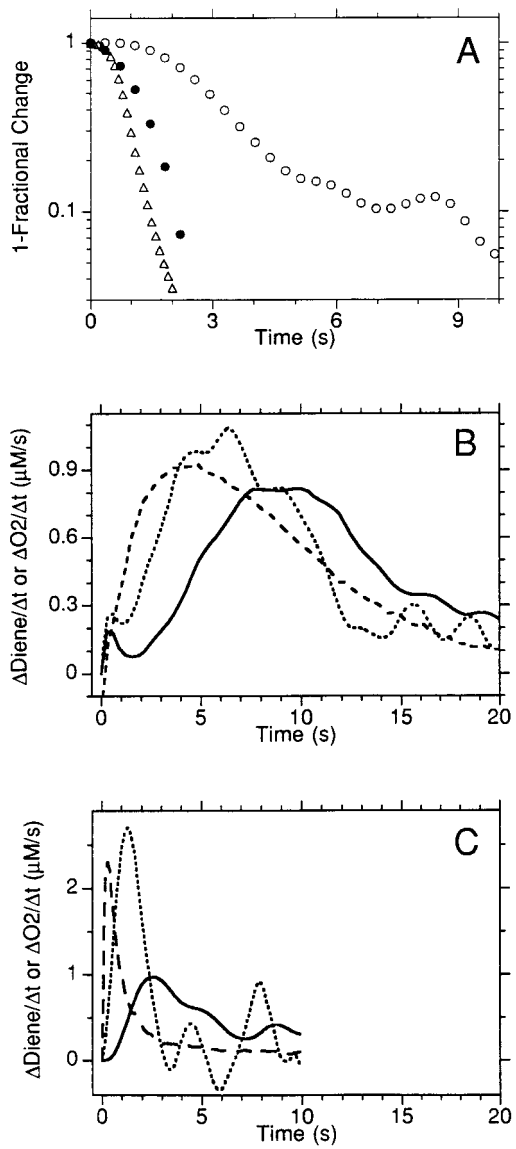


FIGURE 5: Comparison of kinetics of absorbance changes and oxygen electrode response. (A) Injection of anaerobic chromophore solution. Changes in absorbance at 400 nm and oxygen electrode response were monitored simultaneously after injection of 45 $\mu$L of a nitrogen-saturated solution of potassium ferricyanide (4 mg/mL) into an optical cuvette containing 2.8 mL of 0.1 M Tris, pH 8.0, at 25 °C. Fractional changes in absorbance (△) and oxygen electrode response (○) are shown as a function of time after injection. Corrected values for changes in oxygen concentration (●) were calculated using a membrane relaxation rate constant of 0.3 $s^{-1}$. Data from seven separate injections were averaged. (B) Soybean lipoxygenase reaction with 20:2. Velocities of conjugated diene formation (calculated from changes in $A_{235}$; dashed line), uncorrected oxygen electrode response (solid line), and corrected oxygen consumption (dotted line) are shown as a function of time during reaction of 25 $\mu$g enzyme with 13 $\mu$M 20:2 under the conditions described for panel A. Data from four reactions were averaged. (C) PGHS reaction with 20:2. Velocities of conjugated diene formation (calculated from changes in $A_{235}$; dashed line), uncorrected oxygen electrode response (solid line), and corrected oxygen consumption (dotted line) are shown as a function of time during reaction of 160 nM enzyme with 19 $\mu$M 20:2 under the conditions described for panel A. Data from six reactions were averaged. Other details are given under Materials and Methods.

formation are almost superimposable, with about a 1.1 ratio between the peak corrected oxygen uptake velocity and the peak velocity of diene formation (Figure 5B). Coincident kinetics of oxygen uptake and diene formation, with a stoichiometry of 1, are expected from the generally accepted reaction mechanism for the lipoxygenase reaction (*24*).

Oxygen consumption and hydroperoxide product formation were also monitored simultaneously during reaction of PGHS with 20:2 (Figure 5C). The diene formation rate accelerated very rapidly, reaching a peak of 2.3 $\mu$M/s within 1 s. In contrast, the uncorrected oxygen uptake rate peaked at a value of only 1 $\mu$M/s after ~2.5 s of reaction. This large apparent discrepancy of >2-fold between the rates of diene formation and oxygen consumption is resolved by correction of the oxygen electrode data for membrane dampening (Figure 5C). The ratio of the rates of oxygen uptake and diene formation for the reaction of PGHS with 20:2 was about 1.2 (Figure 5C), not very different from that observed with soybean lipoxygenase (Figure 5B).

Correction for membrane dampening had a much larger effect on the oxygen uptake rate for PGHS than for lipoxygenase (Figure 5B,C). This is a consequence of the faster acceleration and deceleration of oxygen uptake in PGHS compared to lipoxygenase. The time frame of the PGHS reaction (1−2 s) is shorter than the relaxation time constant of the membrane (~3 s), resulting in severe attenuation, whereas the lipoxygenase reaction takes 4 s to peak and then persists, permitting the electrode response to more closely track the changes in oxygen level. The velocity calculated from the uncorrected electrode signal underestimates the true cyclooxygenase rate by a factor of ~2, even though the uncorrected velocity provides a reasonable estimate of the lipoxygenase rate (Figure 5B,C and ref 11). Calibration of the electrode signal using lipoxygenase reactions (*9*) thus does not reveal the need to correct the electrode signal when cyclooxygenase velocities in rapidly accelerating PGHS reactions are calculated. The raw cyclooxygenase velocity used in the present experiment with 20:2 in Figure 5C (1 $\mu$M $O_2$/s) falls within the range of 0.2−1.1 $\mu$M $O_2$/s reported by Bakovic and Dunford (*9*). Because comparable cyclooxygenase activities were used in these two studies, they have comparable cyclooxygenase acceleration kinetics and membrane dampening effects and require comparable correction of the electrode data to obtain the actual cyclooxygenase velocities. It is important to emphasize that the correction process multiplies the raw velocity by a factor of ~2 for PGHS reactions (Figure 5C). Taking the difference between two uncorrected velocities thus cannot cancel out the membrane dampening effect, contrary to a recent claim (*8*).

*Oxygen/Fatty Acid Stoichiometry for Reaction of PGHS with Arachidonate and 20:2.* The required correction of the oxygen electrode response for membrane dampening magnifies the noise in the electrode signal, making precise determination of the peak velocity difficult (Figure 5B,C). However, correction for membrane dampening is not necessary when the oxygen electrode has time to "equilibrate" with the surrounding solution, such as before the reaction is started and in the late reaction stages when most of the enzyme is self-inactivated. This permits calculation of the overall oxygen consumption during a reaction (termed reaction extent) directly from the oxygen electrode signals at the beginning and end of the reaction. Such measurements of reaction extent were used to obtain more precise estimates of the stoichiometry between oxygen uptake and fatty acid consumption for 20:2 and 20:4 (Figure 6). These reactions included small amounts of fatty acid and excess enzyme, so

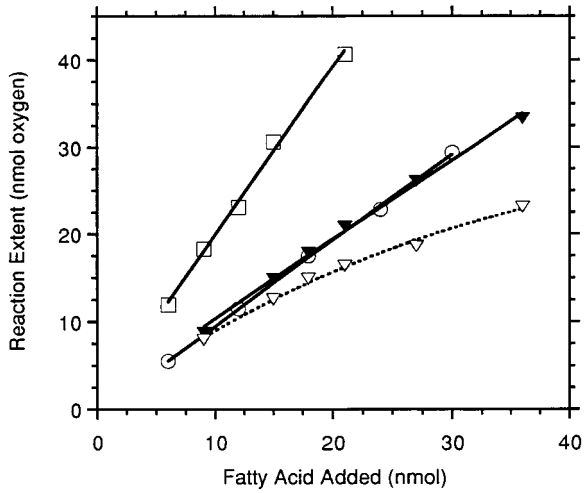


FIGURE 6: Oxygen consumption during reaction of soybean lipoxygenase or PGHS with limiting amounts of 20:2 or 20:4. The final extents of oxygen consumption for the indicated amounts of fatty acid were determined for reactions of soybean lipoxygenase with 20:2 (○), PGHS with 20:4 (□), PGHS with 20:2 (▽), or PGHS with 20:2 in the presence of 100 $\mu$M HOOH (▼). The buffer was 0.1 M potassium phosphate, pH 7.2/1 mM phenol for the PGHS reactions and 0.1 M Tris, pH 8.5/1 mM phenol for the lipoxygenase reactions. The solid lines were fitted by linear regression.

that reaction extent was not limited by self-inactivation. For arachidonate reacted to completion with PGHS, the extent of oxygen consumption was directly proportional to the amount of arachidonate added (Figure 6). The slope of the line fitted to the data had a slope of 1.92 mol of oxygen/mol of arachidonate. This value is in good agreement with the expected stoichiometry of 2 for formation of $PGG_2$.

When 20:2 was reacted with PGHS, the extent of oxygen consumption appeared to be a nonlinear function of the added fatty acid (Figure 6). Addition of 100 $\mu$M hydrogen peroxide at the apparent completion of these reactions resulted in a further burst of oxygen consumption, demonstrating that the initial reaction extent was limited by the hydroperoxide activator level, not by the amount of fatty acid or enzyme. A similar situation has been observed for reaction of PGHS with eicosapentaenoic acid, presumably reflecting a weaker feedback activation loop with eicosapentaenoic acid or 20:2 than with 20:4 (*25*). When the oxygen consumed with 20:2 after addition of hydrogen peroxide was included, the overall extent of oxygen consumption was a linear function of the amount of added 20:2 (Figure 6). The line fitted to the data had a slope of 0.91 mol of oxygen/mol of 20:2. The stoichiometry for reaction of PGHS with 20:2 was thus almost exactly half that observed for reaction with 20:4, just as expected from the observed structures of the respective products (*26*).

For comparison, soybean lipoxygenase was also reacted with limiting amounts of 20:2. Here again, the extent of oxygen consumption was a linear function of the amount of 20:2 added (Figure 6). The slope of the line indicated a stoichiometry of 0.98 mol of oxygen/mol of 20:2, very close to the value of 1 expected. Addition of hydrogen peroxide at the end of the reaction of soybean lipoxygenase with 20:2 or of PGHS with 20:4 did not produce further oxygen uptake (data not shown), demonstrating that the fatty acid level was limiting in these cases.

*Substrate Stoichiometry Measurements in Recent PGHS Mechanistic Studies.* Comparisons of oxygen consumption rates with those for either fatty acid or cosubstrate have been reported in several recent studies of the PGHS mechanism (*7*, *9*−*11*). Some of these studies used oxygen uptake velocities calculated from uncorrected oxygen electrode data. The present results leave no doubt that uncorrected oxygen uptake velocities greatly underestimate the true rates. Thus, substrate stoichiometry ratios based on the uncorrected rates need to be recalculated, and the conclusions drawn from the ratios need to be re-examined.

Two of the studies compared the rate of 20:2 conversion, derived from spectrophotometric measurements, with the rate of oxygen consumption, calculated from uncorrected electrode data (*7*, *9*). A stoichiometry of 2 mol of 20:2 product/mol of oxygen consumed was reported in these studies. This surprisingly high ratio prompted the authors to propose a mechanism that included direct insertion of an oxygen atom into the fatty acid by a tyrosyl radical enzyme intermediate (step h in Scheme 2). Once the oxygen consumption rates are corrected, however, the calculated stoichiometry decreases to ∼1 mol of 20:2 oxygenated/mol of oxygen consumed. A stoichiometry of ∼1.1 can be calculated from the reported absorbance and electrode data at the later stages of one reaction (Figure 2 of ref 7). As mentioned above, the uncorrected electrode signal is much more accurate later in the reaction when the rate of oxygen uptake levels off. Thus, when the electrode characteristics are taken into account, the ratios calculated from the earlier data (*7*, *9*) actually agree well with the stoichiometry of 0.9 obtained in the present reactions with limiting fatty acid (Figure 6). The observed stoichiometric ratio near unity contradicts the combination of dioxygenase and monooxygenase reactions proposed by Bakovic and Dunford (*7*, *9*). On the other hand, the observed ratio is entirely consistent with a conventional dioxygenase reaction. This reassuring outcome indicates that there is no need to reinvestigate the reaction stoichiometry with each of the many other fatty acids which are substrates for PGHS.

In summary, the present results lead to several important conclusions about PGHS substrate stoichiometry. Tyrosyl radical formation in PGHS requires interaction with only 1 equiv of hydroperoxide, consistent with generation of the radical from Compound I by an intramolecular electron transfer. The reported dependence of Compound II formation kinetics on the hydroperoxide level can be explained as an indirect effect rather than reduction of Compound I by hydroperoxide. Accurate quantitation of oxygen uptake kinetics during cyclooxygenase catalysis requires careful correction for the dampening introduced by the oxygen electrode membrane. Comparison of spectrophotometric and corrected oxygen uptake measurements indicates that reaction of PGHS with 20:2 consumes 1 mol of oxygen/mol of oxygenated fatty acid, consistent with a dioxygenase mechanism. These conclusions reduce the complexity of the mechanisms that need to be considered for catalysis by this physiologically important enzyme.

## ACKNOWLEDGMENT

We thank Dr. Graham Palmer (Rice University) for use of the EPR instrument and for assistance in setting up the rapid-freezing apparatus.

## REFERENCES


1. Kulmacz, R. J., and Marshall, P. J. (1988) *Arch. Biochem. Biophys. 266*, 162−170.
2. Picot, D., Loll, P. J., and Garavito, R. M. (1994) *Nature 367*, 243−249.
3. Smith, W. L., Eling, T. E., Kulmacz, R. J., Marnett, L. J., and Tsai, A.-L. (1992) *Biochemistry 31*, 3−7.
4. Tsai, A.-L., Palmer, G., and Kulmacz, R. J. (1992) *J. Biol. Chem. 267*, 17753−17759.
5. Tsai, A.-L., Kulmacz, R. J., and Palmer, G. (1995) *J. Biol. Chem. 270*, 10503−10508.
6. Dietz, R., Nastainczyk, W., and Ruf, H. H. (1988) *Eur. J. Biochem. 171*, 321−328.
7. Bakovic, M., and Dunford, H. B. (1996) *Prostaglandins, Leukotrienes Essent. Fatty Acids 54*, 341−349.
8. Bakovic, M., and Dunford, H. B. (1996) *J. Biol. Chem. 271*, 2048−2056.
9. Bakovic, M., and Dunford, H. B. (1995) *Prostaglandins, Leukotrienes Essent. Fatty Acids 53*, 423−431.
10. Bakovic, M., and Dunford, H. B. (1994) *Biochemistry 33*, 6475−6482.
11. Wei, C., Kulmacz, R. J., and Tsai, A.-L. (1995) *Biochemistry 34*, 8499−8512.
12. Kulmacz, R. J., and Lands, W. E. M. (1987) in *Prostaglandins and Related Substances: A Practical Approach* (Benedetto, C., McDonald-Gibson, R. G., Nigam, S., and Slater, T. F., Eds.) pp 209−227, IRL Press, Washington, DC.
13. Kulmacz, R. J., Tsai, A.-L., and Palmer, G. (1987) *J. Biol. Chem. 262*, 10524−10531.
14. Robinson, J., and Cooper, J. M. (1970) *Anal. Biochem. 33*, 390−399.
15. Kulmacz, R. J., Ren, Y., Tsai, A.-L., and Palmer, G. (1990) *Biochemistry 29*, 8760−8771.
16. Tsai, A.-L., Wei, C., Baek, H. K., Kulmacz, R. J., and Van Wart, H. E. (1997) *J. Biol. Chem. 272*, 8885−8894.
17. Hsuanyu, Y., and Dunford, H. B. (1992) *Arch. Biochem. Biophys. 292*, 213−220.
18. Bakovic, M., and Dunford, H. B. (1995) *Biophys. Chem. 54*, 237−251.
19. Lambeir, A.-M., Markey, C. M., Dunford, H. B., and Marnett, L. J. (1985) *J. Biol. Chem. 260*, 14894−14896.
20. Marquez, L. A., Huang, J. T., and Dunford, H. B. (1994) *Biochemistry 33*, 1447−1454.
21. Dunford, H. B. (1991) in *Peroxidase in Chemistry and Biology* (Everse, J., Everse, K. E., and Grisham, M. B., Eds.) Vol. 2, pp 1−24, CRC Press, Boca Raton, FL.
22. Tsai, A.-L., Kulmacz, R. J., Wang, J.-S., Wang, Y., Van Wart, H. E., and Palmer, G. (1993) *J. Biol. Chem. 268*, 8554−8563.
23. Beechey, R. B., and Ribbons, D. W. (1972) *Methods Microbiol. 613*, 25−53.
24. Yamamoto, S. (1991) *Free Radicals Biol. Med. 10*, 149−159.
25. Kulmacz, R. J., Pendleton, R. B., and Lands, W. E. M. (1994) *J. Biol. Chem. 269*, 5527−5536.
26. Hemler, M. E., Crawford, C. G., and Lands, W. E. M. (1978) *Biochemistry 17*, 1772−1779.
27. Kulmacz, R. J. (1989) *Prostaglandins 38*, 277−288.


BI970397S